Hyperfine Interact
DOI 10.1007/s10751-011-0383-8

Antihydrogen formation by autoresonant excitation of antiproton plasmas

William Alan Bertsche · G. B. Andresen · M. D. Ashkezari · M. Baquero-Ruiz · P. D. Bowe · P. T. Carpenter · E. Butler · C. L. Cesar · S. F. Chapman · M. Charlton · S. Eriksson · J. Fajans · T. Friesen · M. C. Fujiwara · D. R. Gill · A. Gutierrez · J. S. Hangst · W. N. Hardy · R. S. Hayano · M. E. Hayden · A. J. Humphries · J. L. Hurt · R. Hydomako · S. Jonsell · L. Kurchaninov · N. Madsen · S. Menary · P. Nolan · K. Olchanski · A. Olin · A. Povilus · P. Pusa · F. Robicheaux · E. Sarid · D. M. Silveira · C. So · J. W. Storey · R. I. Thompson · D. P. van der Werf · J. S. Wurtele · Y. Yamazaki · ALPHA Collaboration

Abstract In efforts to trap antihydrogen, a key problem is the vast disparity between the neutral trap energy scale ($\sim 50\,\mu$eV), and the energy scales associated with plasma confinement and space charge (~ 1 eV). In order to merge charged particle

W. A. Bertsche (✉) · M. Charlton · S. Eriksson · A. J. Humphries · N. Madsen · D. P. van der Werf
Department of Physics, Swansea University, Swansea SA2-8PP, UK
e-mail: bertsche@cern.ch

G. B. Andresen · P. D. Bowe · J. S. Hangst
Department of Physics and Astronomy, Aarhus University, 8000 Aarhus C, Denmark

M. D. Ashkezari · M. E. Hayden
Department of Physics, Simon Fraser University, Burnaby BC, V5A 1S6, Canada

M. Baquero-Ruiz · S. F. Chapman · J. Fajans · A. Povilus · C. So · J. S. Wurtele
Department of Physics, University of California, Berkeley, CA 94720-7300, USA

P. T. Carpenter · J. L. Hurt · F. Robicheaux
Department of Physics, Auburn University, Auburn, AL 36849-5311, USA

E. Butler
Physics Department, CERN, 1211 Geneva 23, Switzerland

C. L. Cesar
Instituto de Física, Universidade Federal do Rio de Janeiro, Rio de Janeiro 21941-972, Brazil

T. Friesen · R. Hydomako · R. I. Thompson
Department of Physics and Astronomy, University of Calgary, Calgary AB, T2N 1N4, Canada

species for direct recombination, the larger energy scale must be overcome in a manner that minimizes the initial antihydrogen kinetic energy. This issue motivated the development of a novel injection technique utilizing the inherent nonlinear nature of particle oscillations in our traps. We demonstrated controllable excitation of the center-of-mass longitudinal motion of a thermal antiproton plasma using a swept-frequency autoresonant drive. When the plasma is cold, dense and highly collective in nature, we observe that the entire system behaves as a single-particle nonlinear oscillator, as predicted by a recent theory. In contrast, only a fraction of the antiprotons in a warm or tenuous plasma can be similarly excited. Antihydrogen was produced and trapped by using this technique to drive antiprotons into a positron plasma, thereby initiating atomic recombination. The nature of this injection overcomes some of the difficulties associated with matching the energies of the charged species used to produce antihydrogen.

Keywords Antihydrogen · Plasma · Nonlinear · Dynamics

M. C. Fujiwara · D. R. Gill · L. Kurchaninov · K. Olchanski · A. Olin · J. W. Storey
TRIUMF, 4004 Wesbrook Mall, Vancouver BC, V6T 2A3, Canada

A. Gutierrez · W. N. Hardy
Department of Physics and Astronomy, University of British Columbia,
Vancouver BC, V6T 1Z4, Canada

R. S. Hayano
Department of Physics, University of Tokyo, Tokyo 113-0033, Japan

S. Jonsell
Department of Physics, Stockholm University, 10691 Stockholm,
Sweden

S. Menary
Department of Physics and Astronomy, York University,
Toronto ON, M3J 1P3, Canada

P. Nolan · P. Pusa
Department of Physics, University of Liverpool, Liverpool L69 7ZE, UK

E. Sarid
Department of Physics, NRCN-Nuclear Research Center Negev,
Beer Sheva, 84190, Israel

D. M. Silveira · Y. Yamazaki
Atomic Physics Laboratory, RIKEN Advanced Science Institute,
Wako, Saitama 351-0198, Japan

J. S. Wurtele
Lawrence Berkeley National Laboratory, Berkeley, CA 94720, USA

Y. Yamazaki
Graduate School of Arts and Sciences, University of Tokyo,
Tokyo 153-8902, Japan

1 Autoresonance dynamics

When a swept frequency drive is applied to a nonlinear oscillator, the response can become phase-locked to the drive. When this happens, the oscillator's amplitude can be controlled directly by the frequency of the drive. This phenomenon, known as autoresonance, occurs in a wide variety of driven nonlinear oscillators from plasma modes [5] to orbital dynamics [7]. We recently demonstrated that autoresonance can be used to controllably excite a cold, dense antiproton plasma [4]. The excitation dynamics can be largely independent of the initial condition of the antiprotons and the positrons. This feature makes the technique useful for injecting antiprotons into positrons, as it is robust against small fluctuations in the initial plasmas.

A confined antiproton plasma with charge $-e$ and mass m, confined on the z-axis by the strong magnetic field pointing in the z direction experiences an electrostatic potential that can be approximated (at low antiproton energy) as $\Phi(z) \approx -\Phi_0\big(1 - \cos(kz)\big) - E_d z \cos\left(\int \omega dt\right)$, where E_d is a uniform, time-varying drive field. The quantities Φ_0, k, and E_d are found by fitting to the actual potentials used in our measurements. Defining $\theta = kz$, $\bar{\epsilon}$ to be a normalized drive amplitude, and allowing the drive frequency ω to be time-dependent with a sweep (chirp) rate magnitude α and initial frequency ω_i, the equation of motion is:

$$\ddot{\theta} + \omega_0^2 \sin\theta = \bar{\epsilon} \cos\left(\omega_i t - \alpha t^2/2\right). \tag{1}$$

This is the same equation as that of a uniformly driven, nonlinear pendulum with a linear (small-amplitude) oscillation frequency of $\omega_0 = \sqrt{ek^2\Phi_0/m}$.

Autoresonance control of an oscillator requires an anharmonic potential with a monotonic relationship between the amplitude and response frequency. In the case of antiprotons electrostatically confined next to a positron plasma, the oscillation in question is the longitudinal bounce frequency ω_b of an antiproton with total energy $U = mv_z^2/2 - e\Phi(z)$ in its well, where:

$$\frac{\pi}{\omega_b(U)} = \int_{z_l}^{z_r} \frac{dz}{|v_z|}, \tag{2}$$

Autoresonant excitation, in the pendulum case, takes place by sweeping the frequency of the drive from above the linear frequency ω_0 down to a final frequency. If sweep-rate α and drive amplitude $\bar{\epsilon}$ meet a chirp-rate / amplitude threshold [8]:

$$\bar{\epsilon} \geq 8\sqrt{\omega_0}\left(\frac{\alpha}{3}\right)^{3/4}, \tag{3}$$

the oscillator will phase-lock to the drive as it passes through the linear frequency. When this happens, it will match its response frequency and hence excitation amplitude to the drive frequency through the relationship described by (2).

Figure 1 shows a typical set of potentials and bounce frequency–energy relationships for antiprotons in the ALPHA experiment. The presence of positrons significantly alters the electrostatic potential. In order to accurately calculate the full potential Φ, the positron plasma must be characterized by measuring its profile, number [3], and temperature [6]. It is then possible to solve the Poisson–Boltzmann equation to determine the self-consistent charge density $n(z)$ [11]. We neglect the influence of antiprotons on the potential since, in the ALPHA experiment, there are typically far fewer of them than positrons.

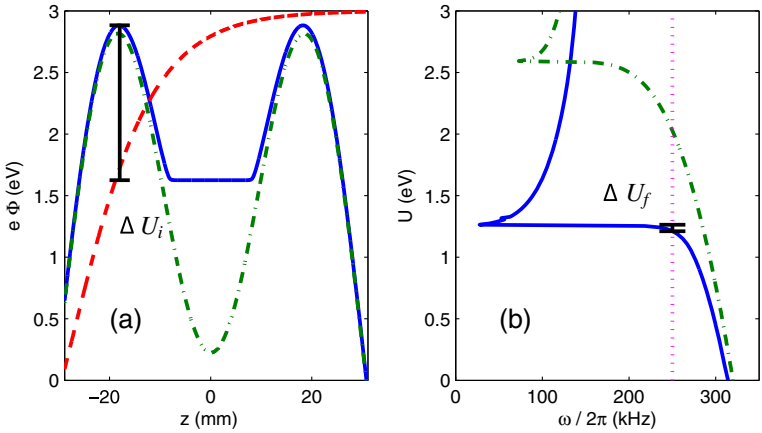

Fig. 1 **a** Potentials for plasma conditions typical of antihydrogen production in the ALPHA experiment. The *green dot-dash curve* shows the vacuum potential, while the *solid blue curve* shows the self-consistent potential for a positron plasma with $\sim 2 \cdot 10^6$ particles, radius of ~ 2 mm, and a temperature of ~ 100 K. The *dashed red line* is a $\times 100$ amplification of a the typical drive potential. Antiprotons originate in the potential well centered on -18 mm. **b** The antiproton bounce frequencies calculated for the two confining potentials in (**a**). The *dotted magenta line* marks 250 kHz, a typical drive final frequency. Electrostatic injection energy ΔU_i and autoresonant injection energy offset ΔU_f are marked with black brackets in (**a**) and (**b**) respectively

2 Injection by autoresonant excitation

Antihydrogen was first formed by direct recombination of charged clouds of antiprotons and positrons confined in a double well potential [1, 9]. In these early antihydrogen production schemes, antiprotons were injected from the side by spilling them out of a confining potential and allowing them to pass into the positrons while blocking them from escaping the trap altogether. In any injection scheme, there is an energy difference ΔU_i that is the potential energy confining the positrons in the final double-well configuration (indicated in Fig. 1a). The antiprotons require at least this much total energy in the final well configuration in order to pass through positrons. In the side-injection scheme, antiprotons are ejected from a separate electrostatic well and ideally end with exactly ΔU_i in the final potential.

Autoresonant injection drives initially cold antiprotons to this energy level by sweeping the drive to a low frequency; in doing so, the antiprotons gain longitudinal energy towards the positron confinement ΔU_i, as illustrated in Fig. 1b. Naively, one might assume this scheme would never work, because the energy at which antiprotons would pass into positrons corresponds to an impossible frequency of $\omega_b = 0$. However, we experimentally observe that a large fraction of antiprotons are injected before the drive reaches this point. As a consequence, we use an optimization strategy to tune the autoresonance injection final frequency. For a given set of antiproton and positron conditions, we conduct experiments in which we progressively lower the final drive frequency while measuring the number of antihydrogen atoms produced, settling on a frequency which gives us the highest production rate. For the antihydrogen production experiment shown in Fig. 1, this corresponded to a frequency of ~ 250 kHz.

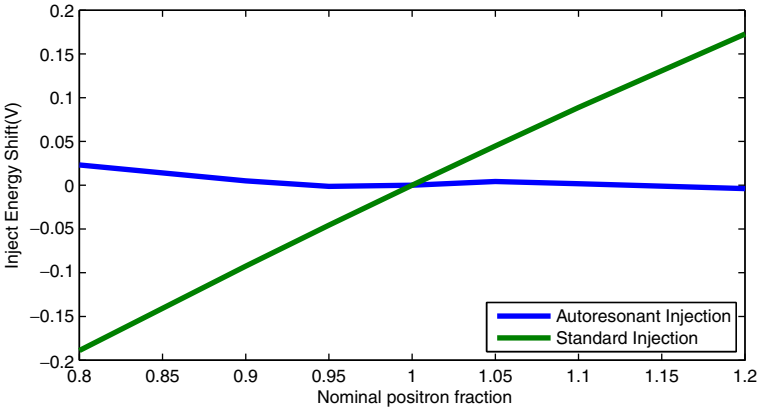

Fig. 2 Energy shift for standard and autoresonant injection schemes. The abscissa is fractional variation from a nominal $N_0 = 2 \cdot 10^6$ positrons. The energy shift shown is $\Delta U_i(N_0) - \Delta U_i$ for the standard injection and $\Delta U_f - \Delta U_f(N_0)$ for autoresonant injection. Antiprotons tuned to ΔU_i injected when there is a negative energy shift do not pass through positrons in the standard injection scheme

While the exact dynamics of the autoresonant injection technique are not well-understood at this time, we can try to establish an energy scale which is related to the accuracy of the autoresonant drive. The final drive frequency is a fixed quantity that corresponds to an energy difference ΔU_f between the space-charge level of the positrons and the final nominal oscillator amplitude (see Fig. 1b).

As a result of the nature of these two energy scales, the autoresonance technique is more stable against positron fluctuations than a side-injection scheme. In a side-injection, the antiproton injection energy must be matched to ΔU_i, a quantity that scales approximately linearly with shot-to-shot changes in positron number. This can be problematic for antihydrogen production: if the space charge decreases, antiprotons will undershoot and not mix with positrons; if it increases, antiprotons will overshoot and have too much energy to form trappable antihydrogen. However, since the boundary for autoresonant injection always corresponds with $\omega_b = 0$, antiprotons will continue to inject, as governed by ΔU_f.

Because of the nonlinear nature of $U(\omega_b)$, ΔU_f is a slower function of positron number than ΔU_i. Figure 2 compares the two energy scales as a function of change in positron number. The fractional change in injection energy is over 10 times less than for conventional injection, and consequently one expects a diminished influence of positron number fluctuations on the outcome of injection.

Another advantage that autoresonant injection has is that mixing is initiated much faster than antiproton-antiproton collisions. Trapped antiprotons have total energy divided into parallel and perpendicular degrees of freedom: $U = -e\Phi(z) + \frac{1}{2}mv_z^2 + \frac{1}{2}m\left(v_x^2 + v_y^2\right)$, where parallel energy is from motion in z and perpendicular energy is from motion in x and y. Coulomb collisions redistribute energy between parallel and perpendicular degrees of freedom, a dynamic that has many consequences for antihydrogen formation [2].

On autoresonant injection, the cold antiprotons predominantly gain parallel energy from the drive. Once excited longitudinally, collisions with other antiprotons

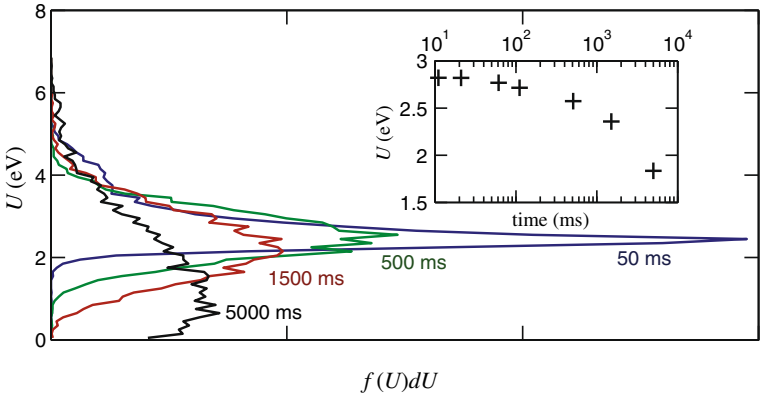

Fig. 3 Antiproton distributions measured at various times after an autoresonant drive

can redistribute parallel energy into the perpendicular degrees of freedom. This has two negative consequences for forming trappable anti-atoms. The first is simply that collisions can move antiprotons into the side wells—these antiprotons are then unavailable for formation unless they are re-injected. The second problem is that collisions, in adding energy to the perpendicular degrees of freedom, will reduce the likelihood of forming trapped antihydrogen.

With the standard side-injection scheme, it can sometimes take seconds for antihydrogen formation to begin because conservatively over-injected antiprotons need time to lose energy in the positrons before antihydrogen formation can take place. Such a delay before mixing means that there is sufficient time for antiprotons to gain perpendicular energy through collisions. Further, this technique has been observed to result in antihydrogen emerging as a hot "beam", as formation takes place before the antiprotons come into equilibrium with positrons [10]. Obviously this is not an ideal outcome as far as trapping antihydrogen is concerned.

We assess the rate at which parallel energy is scattered into perpendicular degrees of freedom by using autoresonance to drive particles to a fixed energy and then measuring the longitudinal energy distribution at various times after the drive ends [4]. Figure 3 shows the results of this sort of measurement. The time scale for energy redistribution in our typical antiproton plasmas used from antihydrogen is a few tens of milliseconds, implying that formation needs to occur faster than this time scale.

In this case, autoresonance also has an advantage. The drive itself is typically around 1 ms in duration, which is far shorter than the measured collisional time scales of the antiprotons in the side well. As the additional kinetic energy of antiprotons passing into positrons is minimized, we expect that less time is needed for collisions with positrons to bring the two species to matching velocities and initiate recombination. We observe that formation using an autoresonant drive is immediate and rapid. This is in contrast with standard side-injection schemes that can take seconds for antihydrogen formation to begin because conservatively over-injected antiprotons need time to lose energy in the positrons before antihydrogen formation takes place. Such a delay before mixing means that there is sufficient time for antiprotons to gain perpendicular energy through collisions.

In conclusion, autoresonance has proved to be a useful tool which allows us to accurately, and efficiently inject antiprotons into positrons, even in the face of small fluctuations in initial plasma parameters. We have just begun investigating the dynamics of this rich process, and there seem to be many possibilities for improving this injection, by, for instance, trying to achieve a low ΔU_f, and thereby reducing excess injection energy in the antiprotons. While the details of the dynamics of the injection process are still not well-understood, we have used this method to produce antihydrogen with sufficiently low energy to be trapped in the ALPHA neutral atom trap.

References

1. Amoretti, M., et al.: Production and detection of cold antihydrogen atoms. Nature **419**, 456–459 (2002)
2. Amoretti, M., et al.: Dynamics of antiproton cooling in a positron plasma during antihydrogen formation. Phys. Lett. B **590**, 133–142 (2004)
3. Andresen, G.B., et al.: Antiproton, positron, and electron imaging with a microchannel plate/phosphor detector. Rev. Sci. Instrum. **80**, 123701 (2009)
4. Andresen, G.B., et al.: Autoresonant excitation of antiproton plasmas. Phys. Rev. Lett. **106**, 025002 (2011)
5. Bertsche, W., Fajans, J., Friedland, L.: Direct excitation of high-amplitude chirped bucket-bgk modes. Phys. Rev. Lett. **91**, 265003 (2003)
6. Eggleston, D.L., Driscoll, C.F., Beck, B.R., Hyatt, A.W., Malmberg, J.H.: Parallel energy analyzer for pure electron plasma devices. Phys. Fluids B **4**, 3432–3439 (1992)
7. Fajans, J., Friedland, L.: Autoresonant (nonstationary) excitation of pendulums, plutinos, plasmas, and other nonlinear oscillators. Am. J. Phys. **69**, 1096–1102 (2001)
8. Fajans, J., Gilson, E., Friedland, L.: Autoresonant (nonstationary) excitation of the diocotron mode in non-neutral plasmas. Phys. Rev. Lett. **82**, 4444–4447 (1999)
9. Gabrielse, G., the ATRAP Collaboration: Background-free observation of cold antihydrogen with field-ionization analysis of its states. Phys. Rev. Lett. **89**, 213401 (2002)
10. Madsen, N., et al.: Spatial distribution of cold antihydrogen formation. Phys. Rev. Lett. **94**(3), 033,403 (2005)
11. Prasad, S.A., O'Neil, T.M.: Finite length thermal equilibria of a pure electron-plasma column. Phys. Fluids **22**, 278–281(1979)